PLOS ONE

RESEARCH ARTICLE

FluidFM as a tool to study adhesion forces of bacteria - Optimization of parameters and comparison to conventional bacterial probe Scanning Force Spectroscopy

Linda Hofherr, Christine Müller-Renno*, Christiane Ziegler

Department of Physics and Research Center OPTIMAS, University of Kaiserslautern, Kaiserslautern, Germany

* cmueller@physik.uni-kl.de

OPEN ACCESS

Citation: Hofherr L, Müller-Renno C, Ziegler C (2020) FluidFM as a tool to study adhesion forces of bacteria - Optimization of parameters and comparison to conventional bacterial probe Scanning Force Spectroscopy. PLoS ONE 15(7): e0227395. https://doi.org/10.1371/journal.pone.0227395

Editor: Kerstin G. Blank, Max-Planck-Institut fur Kolloid und Grenzflachenforschung, GERMANY

Received: December 15, 2019

Accepted: May 28, 2020

Published: July 6, 2020

Data Availability Statement: All relevant data are within the paper.

Funding: Funded by the Deutsche Forschungsgemeinschaft (DFG, German Research Foundation) – Project-ID 172116086 – SFB 926. The funders had no role in study design, data collection and analysis, decision to publish, or preparation of the manuscript.

Competing interests: The authors have declared that no competing interests exist.

Abstract

The FluidFM enables the immobilization of single cells on a hollow cantilever using relative underpressure. In this study, we systematically optimize versatile measurement parameters (setpoint, z-speed, z-length, pause time, and relative underpressure) to improve the quality of force-distance curves recorded with a FluidFM. Using single bacterial cells (here the gram negative seawater bacterium *Paracoccus seriniphilus* and the gram positive bacterium *Lactococcus lactis*), we show that Single Cell Force Spectroscopy experiments with the FluidFM lead to comparable results to a conventional Single Cell Force Spectroscopy approach using polydopamine for chemical fixation of a bacterial cell on a tipless cantilever. Even for the bacterium *Lactococcus lactis*, which is difficult to immobilze chemically (like seen in an earlier study), immobilization and the measurement of force-distance curves are possible by using the FluidFM technology.

Introduction

Although often unwanted, biofilms can also be applied in biofilm reactors, for example in ethanol and butanol production or newly developed biofilm-based fuel cells [1–3]. In this study, we focus on the FluidFM for assessing adhesion forces of productive bacteria to surfaces, which is a key step in biofilm formation. Scanning Force Microscopy (SFM) and Scanning Force Spectroscopy (SFS) are versatile methods to study bacterial adhesion on surfaces. More specifically, single cell force spectroscopy (SCFS) is a prominent method to study the interaction of a single (bacterial) cell with a surface. Conventionally, a chemical functionalization of the SFM's cantilever is used to immobilize a single bacterium for means of SCFS. However, due to different properties of bacteria, various functionalizations like polydopamine [4–6], poly-L-lysine [7–10], Cell-Tak [10, 11] or glutaraldehyde [9, 12, 13] are used for different cells, making it necessary to test and find a suitable immobilization method for each cell type.

Some years ago, the FluidFM was introduced as an alternative method for the immobilization of cells on a cantilever [14]. The FluidFM is an add-on for conventional SFMs and allows

the application of underpressure at the aperture of a hollow cantilever, which serves as micro- or nanopipette. For this purpose, the cantilever is filled with a liquid and coupled to a pumping unit, enabling a variation of the pressure inside the cantilever compared to the environment. By applying an underpressure relative to the environment, it is possible to draw a cell towards the opening of the cantilever and retain it there. The FluidFM has been used to study the elasticity and adhesion of several cell types [15–18]. Studies addressing specifically the adhesion of bacterial cells include the work of Potthoff *et al.* [19], Sprecher *et al.* [20] and Mittelviefhaus *et al.* [21]. Potthoff *et al.* further showed that bacteria still divided after SCFS measurements using the FluidFM and thus had survived the measurement.

In this study, we determine how different measurement parameters like setpoint, z-speed, z-length, pause time, and relative underpressure influence the shape and quality of force-distance curves in a SCFS experiment using FluidFM. For this purpose, we studied two productive bacteria: The gram positive lactic acid bacterium *Lactococcus lactis*, which is applied in dairy industry as well as in the production of the antibacterial peptide nisin [22], and the gram negative seawater bacterium *Paracoccus seriniphilus* which produces the enzyme serine dehydratase [23].

While focusing on the FluidFM, we implement measurement parameters for an SCFS measurement routine for *Lactococcus lactis*. A previous study showed that none of the typically used chemical immobilization methods leads to a reliable attachment of the cells without at the same time changing their surface properties [24]. Therefore, we used the FluidFM to physically immobilize the bacteria on the opening of a FluidFM cantilever and determined parameters for recording force-distance curves.

Further, we used the well-studied gram negative bacterium *Paracoccus seriniphilus* in terms of SCFS [25] to compare the immobilization by means of FluidFM with the well-established immobilization with polydopamine.

Materials and methods

Bacterial growth conditions

The spherical, gram positive lactic acid bacterium *Lactococcus lactis* subsp. *lactis* was grown in DSMZ medium 11 (Leibniz Institute DSMZ–German Collection of Microorganisms and Cell Cultures). Both bacteria have a size of 0,5–1 μm. The spherical, gram negative seawater bacterium *Paracoccus seriniphilus* was grown in complex medium as described elsewhere [26]. For both strains, precultures were incubated for 17 hours at 30˚ C. Afterwards, the precultures were diluted and kept at 30˚ C for another 24 hours before they were diluted in 0.9% NaCl solution for subsequent SCFS measurements. During the immobilization of the cell on the cantilever, the volume of the droplet on the glass surface and therefore the OD within the droplet changed constantly due to evaporation of water from the droplet. To prepare the initial solution, one drop of bacterial liquid culture was added to roughly 10 ml 0.9% NaCl solution.

Sample preparation

Glass samples (microscope glass, Thermo Scientific, soda-lime glass) were cleaned by subsequent immersion in acetone, isopropanol and distilled water in an ultrasonic bath for 10 min each (in the following referred to as "standard cleaning").

Titanium samples were obtained from Deutsche Titan GmbH (Thyssen Krupp, Essen, Germany) and polished by the metal workshop of the University of Kaiserslautern, Germany, by lapping with diamond paste (6 μm, Joke company, Germany) and applying diamond paper (diamond fine polishing suspension, 3 and 1 μm, Joke company, Germany). The day before use, titanium samples were cleaned by standard cleaning and subsequent plasma cleaning (O_2,

5 min, 50 W, and 0,3 mbar, Electronic Diener, Ebhausen, Germany) as described in Fingerle *et al.* [27].

Polished stainless austenitic steel samples (1.4571, X6CrNMoTi17-12-2) were used one day after a base and acid cleaning with 2% NaOH solution (JT Baker Organic Reagent Chemicals, Phillipsburg, USA) and 2% HNO_3 solution (65%, JT Baker Organic Reagent Chemicals, Phillipsburg, USA) as described by Huttenlochner *et al.* [28]. After base and acid cleaning, samples were standard cleaned as described above.

Single cell/particle force spectroscopy

All measurements were performed with a Nanowizard III assembled with a FluidFM add-on (Cytosurge, Switzerland), positioned under an acoustic hood (both JPK Instruments AG, D) and mounted on an active vibration isolation system (Halcyonics-i4, Accurion GmbH, Germany) to minimize the effects of environmental vibrations. Additionally, the Nanowizard III is mounted on an inverted microscope (AxioObserver A1, Zeiss, Germany) to observe the cells and to address the bacteria to be approached with the tip. A droplet of diluted bacterial solution was placed on a microscope glass. For SCFS (single cell force spectroscopy), a FluidFM nanopipette (Cytosurge, Switzerland) with an aperture of 300 nm and a spring constant of 0.28–0.52 N/m was filled with glycerol, calibrated by the contact-based thermal noise method [29, 30] and brought in close proximity to the glass surface. By applying a pressure of -800 mbar compared to the environment, a single bacterium was drawn to the aperture of the cantilever. For subsequent measurements, the negative pressure was reduced to smaller values. The bacteria were then transferred to the substrate of interest.

Alternatively, All-In-One-Tipless Cantilevers A (BudgetSensors, Bulgaria) with a spring constant of 0.22 N/m were cleaned and functionalized with polydopamine (for details, see [5]). After functionalization, the cantilever was pressed onto a single bacterium for 3 min with a setpoint of 2 nN to bind the cell to the cantilever.

All force-distance curves of *Paracoccus seriniphilus*, both for FluidFM and conventional SCFS, were recorded in liquid (0.9% NaCl) with a setpoint of 2 nN, a z-length of 2 μm and a z-speed of 2 μm/s. For *Lactococcus lactis*, we varied measurement parameters until we found a setpoint of 5 nN, a z-length of 0.5 μm and a z-speed of 5 μm/s to be appropriate parameters to determine the adhesion force on glass. The given adhesion force was determined by the largest force relative to the baseline. A discrimination between a rupture force and the largest force was not necessary because the bacterial Fluid FM probe does not show a tip interaction peak.

We discarded curves when:

- they were not completely resolved
- showed no fittable/nearly constant baseline
- no adhesion peak was distinguishable from the baseline

The ratio of the analyzable force-distance curves was calculated by the number of usable force-distance curves (number of measured force-distance curves minus number of discarded curves) divided by the number of measured force-distance curves.

For the measurements with polystyrole particles monodisperse Polybead® microspheres 1.00 μm (Polysciences, Inc., USA) with a size distribution from 0.90–1.10 μm were used. Polybead® Microspheres are packaged in an 2.5% solids (w/v) aqueous suspension with minimal surfactant in the final preparation.

All given data points are representing the mean value of several measured values (analyzable force-distance curves) at the same conditions. The error bars represent the standard deviation of the values used for the mean values.

Results and discussion

Influence of measurement parameters on the adhesion force of a blank nanopipette

We evaluated the influence of the setpoint, the z-speed and the applied pressure on the adhesion force of a blank FluidFM nanopipette with a spring constant of 0.52 N/m on a glass surface. The goal of these measurements was to distinguish the effects we observe with bacteria from those which originate from the nanopipette itself.

Fig 1A and 1B shows the course of the adhesion force of a blank nanopipette as a function of the setpoint (a) and the z-speed (b) without pressure applied. Whereas the adhesion force increases with an increasing setpoint up to 20 nN, there is no clear trend for the z-speed without pressure and with a pressure of -50 mbar. However, the absolute values of the adhesion force are slightly higher with than without applied pressure. Besides setpoint and z-speed, we determined the adhesion forces of a blank nanopipette as a function of the applied pressure for two different sets of parameters (see Fig 1C). The two sets of parameters match the ones used in the further course of the paper where the adhesion of single bacterial cells is investigated. In addition the straight line for the suction force (according to [19]) is shown in Fig 1C. It can be seen that for both sets of parameters the adhesion forces follow the line of the suction force for negative pressure. This is in line with the fact that the blank nanopipette shows a neglectable adhesion force at 0 mbar. For positive pressure, the adhesion forces are slightly smaller than the suction force, because now the overpressure repels the tip from the surface. In contrast to the subsequent measurements with bacteria, all recorded force-distance curves were of good quality for evaluation. The detected small variations most probably originate from pressure variations due to imperfections of the pipette opening and the stability of the pump. The shape of the curves is very similar to force-distance curves recorded with a conventional blank tip and shows a single sharp detachment event.

Influence and optimization of FluidFM measurement parameters

We investigated the influence of the parameters setpoint, z-length, z-speed, and pause time on the shape and quality of force-distance curves recorded by FluidFM. The investigation of each parameter was conducted using the optimized parameters determined before.

First, we studied the impact of the setpoint on the adhesion force and the quality of the force-distance curves. We found a clear correlation between the setpoint and the number of analyzable force-distance curves between 2 and 20 nN setpoint (2 nN, 3.5 nN, 5 nN, 7.5 nN, 10 nN, 15 nN, 20 nN; Fig 2) at 1μm z-length, 2 μm/s z-speed and 10 s pause time. Further, we found that the adhesion force increases with the setpoint, meaning the adhesion force strongly depends on the applied force. This increase is expected because of a larger contact area of the bacterium with the surface.

Fig 3 shows a set of 10 typical force-distance curves recorded with a relatively small setpoint of 2 nN. It can be seen that the trace varies substantially (Fig 3 left) while the baseline of the retrace (Fig 3 right) was set to 0 nN. Due to the hydrodynamic drift between approach and retract, the contact area of the retraction curve is not completely displayed for small setpoints. Further, the retract part shows a large drift in the area of the interaction-free sector, both being an indicator for a setpoint too small. Fig 4 shows a set of 10 typical force-distance curves with a

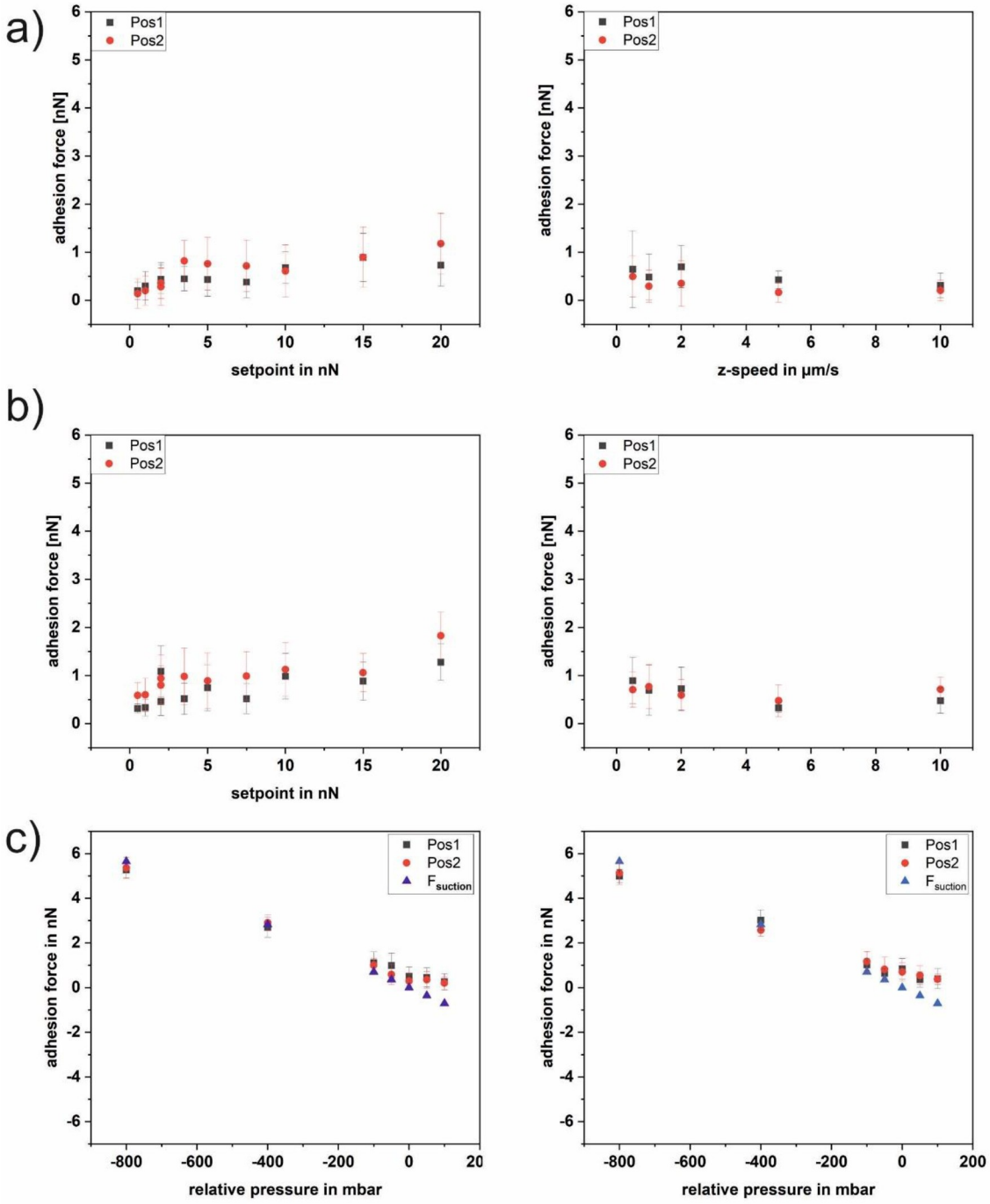

Fig 1. Adhesion force of a blank FluidFM nanopipette on glass. Each data point comprises 25 force-distance curves. a) no pressure (0 mbar) applied. Left as a function of the setpoint, right as a function of the z-speed. b) pressure of -50 mbar applied;. Left as a function of the setpoint, right as a function of the z-speed. c) as a function of applied pressure. Two different sets of parameters were used. Left setpoint 2 nN, z-speed 2 µm/sec, right setpoint 5 nN, z-speed 5 µm/sec, both including the curve for $F_{suction}$ calculated according to [19].

https://doi.org/10.1371/journal.pone.0227395.g001

more stable baseline, recorded with a setpoint of 10 nN. The hydrodynamic drift still exists, but the curves themselves are much more stable. After the optimization of the other parameters like z-speed and z-length (see further discussion of the paper), the force distance curves

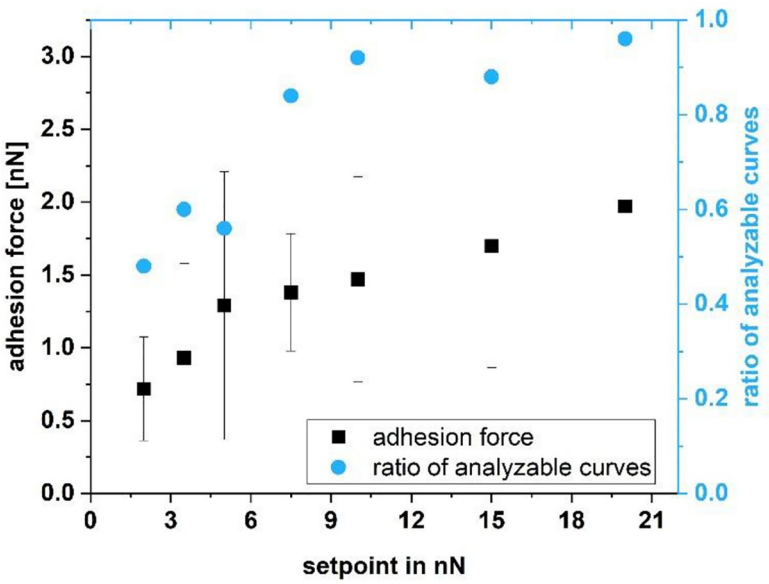

Fig 2. Adhesion force and ratio of analyzable force-distance curves of a single *Lactococcus lactis* cell on glass as a function of the setpoint; each data point comprises 25 force-distance curves.

https://doi.org/10.1371/journal.pone.0227395.g002

were again optimized in relation to the setpoint. For 0.5 μm, a z-speed of 5 μm/sec and a pause time of 10 s a setpoint of 5 nN showed the same quality and ratio of analyzable curves than before the parameter set with a setpoint of 10 nN. Because the setpoint should be as small as possible to avoid stressing the cells, a setpoint of 5 nN was finally chosen. This analysis shows, that an iterative optimization of all parameters is a good lab routine.

For the z-length, the parameters 0.5, 1 and 2 μm were tested (at -100 mbar pressure, 5 nN setpoint, 2 μm/s z-speed and 10 s pause time). 0.5 μm were most suitable, because for higher z-lengths the drift between approach and retract baseline increased and the baselines became unsteady. We determined that the quality of the force-distance curves increases with a decreasing z-length. Still, it is mandatory for the z-length to cover all rupture events. Especially when changing the surface material or the type of cells, it is mandatory to adjust the z-length to

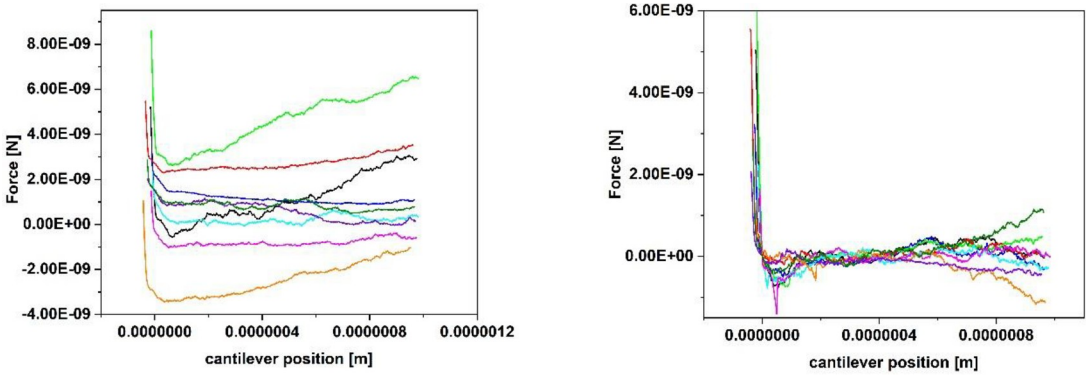

Fig 3. 10 typical force-distance curves (left trace, right retrace., the baseline of all the retrace curves was set to 0 nN) of a single *Lactococcus lactis* cell on glass, recorded with the following parameters: Setpoint 2 nN, z-length 1 μm, z-speed 2 μm/s, pause time 10 s.

https://doi.org/10.1371/journal.pone.0227395.g003

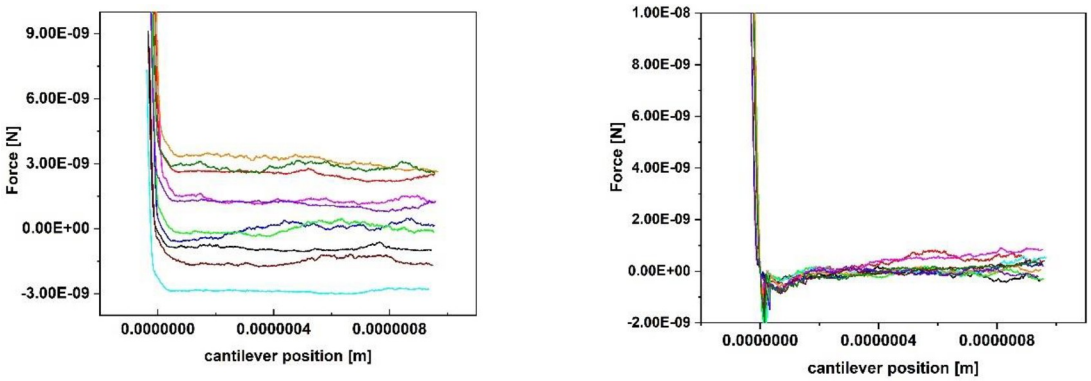

Fig 4. 10 typical force-distance curves (left trace, right retrace. The baseline of all the retrace curves was set to 0 nN) of a single *Lactococcus lactis* cell on glass, recorded with the following parameters: Setpoint 10 nN, z-length 1 μm, z-speed 2 μm/s, pause time 10 s.

https://doi.org/10.1371/journal.pone.0227395.g004

cover all rupture events. Since the z-length of 0.5 μm was enough to catch all breaking events between cell and surface, we sticked to the smallest of these lengths.

For the z-speed, we applied values between 0.5 and 10 μm/s (0.5 μm/s, 1 μm/s, 2 μm/s, 5 μm/s, 10 μm/s at -100 mbar pressure, 0.5 μm z-length, 10 s pause time and 5 nN setpoint). Whereas small z-speeds cause the approach and retract curves to diverge as seen for the optimization of the contact time (see Fig 5), this effect is smaller at higher z-speeds. For smaller z-speeds (0.5 and 1 μm/sec) the baseline became unstable. This effect decreases with increasing the z-speed and is not visible for 5 and 10 μm/sec. We have choosen the slowest speed delivering good curves to minimize the stress for the cells. Therefore, the z-speed should be increased to the point where divergance is minimized. For our setup, this was 5 μm/s. In addition, we investigated the effect of viscoelasticity when the z-speed is increased as described in [26]. For all the investigated values of the z-speed the elasticity stays unchanged within the error bars. All the following measurements were thus taken in the purely elastic regime.

Further, we studied the influence the pause time has on the shape of force-distance curves of *Lactococcus lactis*. For this purpose, we applied pause times between 0.5 and 300 s between approach and retract curves (0.5 s, 1 s, 2 s, 5 s, 10 s, 20 s, 60 s and 300 s at 5 nN setpoint, 0.5 μm z-length and 5 μm/s z-speed). With a pause time larger than 2 s, typical bacterial rupture events

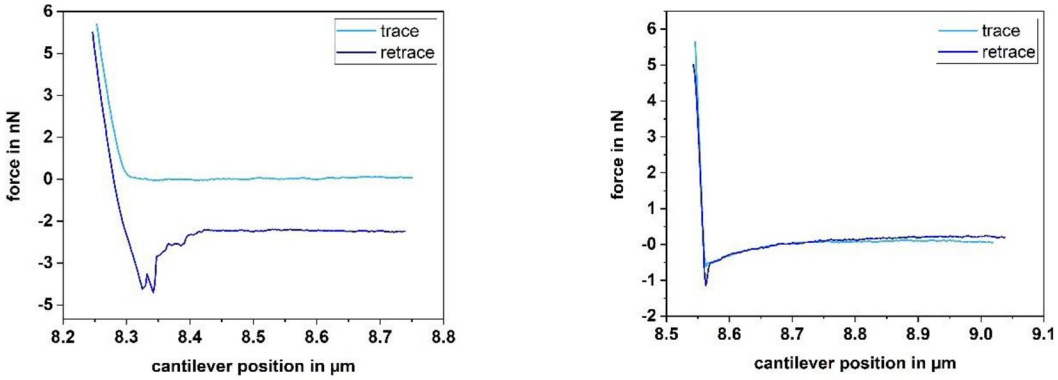

Fig 5. Force-distance curves of a single *Lactococcus lactis* cell on glass, recorded with the following parameters: Left: Setpoint 5 nN, z-length 0.5 μm, z-speed 5 μm/s, pause time 300 sRight: Setpoint 5 nN, z-length 0.5 μm, z-speed 5 μm/s, pause time 0.5 s.

https://doi.org/10.1371/journal.pone.0227395.g005

are observable (see Fig 5 left). For pause times shorter than 2 s, the curves change their appearance and show a single sharp rupture event and a curvature in the baseline (see Fig 5 right). This behavior is reversible, meaning that by increasing the pause time, the bacterial rupture events reappear and the baseline straightens. Further, a longer pause time often correlates with an offset between approach and retract. However, this offset does not disturb the determination of the adhesion force as long as the curve is completely displayed.

The parameters with which the force-distance curves are recorded play an important role when determining adhesion forces by SCFS. By determining suitable parameters for recording force-distance curves with *Lactococcus lactis*, we found the adhesion force increasing with the setpoint (see Fig 2). To summarize, for *Lactococcus lactis* in combination with the FluidFM, we found a setpoint of 5 nN, a z-length of 0.5 μm and a z-speed of 5 μm/s to be appropriate parameters to determine the adhesion force on glass, thus showing that the FluidFM is suitable for the immobilization of a single *Lactococcus lactis* bacterium and subsequent SCFS measurements, which had not been possible in a reliable way without changing the cell's properties previously.

For investigating the force-distance curves of the gram negative bacterium *Paracoccus seriniphilus*, we applied a setpoint of 2 nN, a z-length of 2 μm and a z-speed of 2 μm/s since these parameters yield force-distance curves of good quality for both the FluidFM and the chemical immobilization approach using polydopamine (see next section). Concerning *Paracoccus seriniphilus*, we investigated how the applied pressure used for the immobilization by FluidFM influences the adhesion force between bacterium and surface. From Fig 6 we conclude that the influence of the applied pressure is small compared to a decrease of the adhesion force with a growing number of force-distance curves recorded. Referring to the literature, the decrease in the adhesion force for the repeated contact between cell and surface is due to irreversible bonds [31]. Once broken, these bonds are unable to contribute to the adhesion force between cell and surface when recording subsequent force-distance curves, thus leading to a continuous decrease.

Once in Fig 6B the gradient due to the number of recorded force-distance curves decreased, the adhesion force for -20, -50 and 0 mbar exceeds the neighboring values which were recorded with higher suction force. Nevertheless, taking into account the error bars of the data points following -40 mbar, these changes could as well be due to the variance within the 25 force-distance curves recorded for each pressure. Since the cell is not held at the tip via underpressure when applying 0 mbar, we suggest that additional attractive forces act between the cells and the material of the nanopipette at the rim of the opening.

Further, since each data point in Fig 6 was recorded on a separate position on the glass surface, we conclude that the decreasing adhesion force due to repeated recording of force-distance curves at least partly results from changes of the interaction partner immobilized on the nanopipette. In Fig 6, this partner is the bacterial cell. To investigate if the changes in the cells are due to properties connected to the living nature of the bacterial cell, we expanded the measurements to polystyrene particles (Polybead Microspheres 1.00 μm, Polysciences, USA) instead of living cells. As can be seen in Fig 7, the decrease is not due to any malfunction or active adaptation of the biological component but can be observed for the elastic inanimate polystyrene particle as well. The decay in the force thereby is similar to the one observed by Dörig *et al.* [18]. However, they studied the repeated contact between an avidin-coated bead and a PLL-g-PEG-biotin-coated surface and thus used functionalized surfaces. While the stripping of molecules from the surface was given as an explanation for the decay of contact adhesion in the paper of Dörig et al., this cannot be the explanation here since we did not use functionalized surfaces. We therefore conclude that this effect at least partially originates from

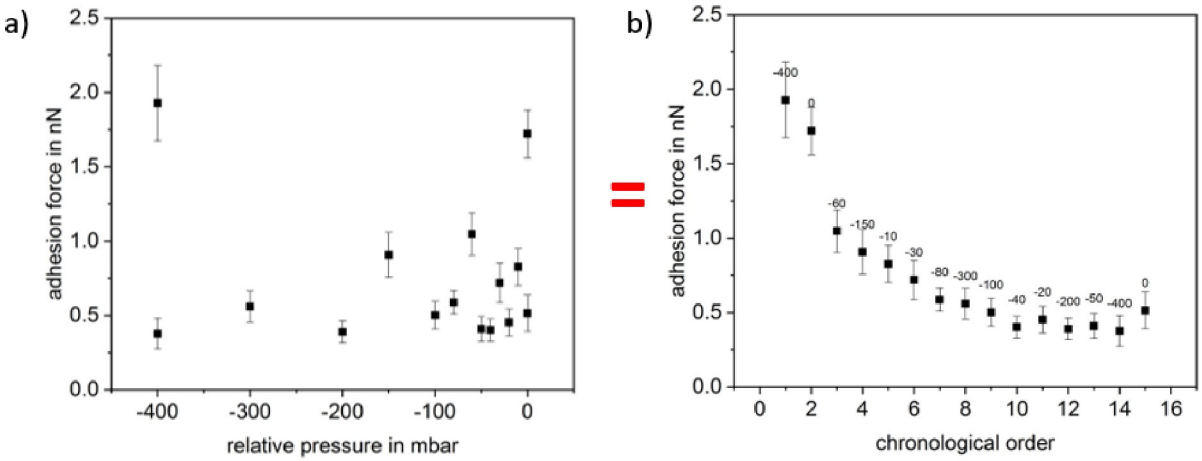

Fig 6. Adhesion force of *Paracoccus seriniphilus* on glass in a FluidFM experiment. Both, a and b, show the same data set, either sorted according to the applied pressure (a) or in chronological order (b); each data point comprises 25 force-distance curves.

https://doi.org/10.1371/journal.pone.0227395.g006

the measurement process itself, e.g. a small leak between the syringe rim and the particle which widens with time.

Besides studying the influence of the applied pressure, we recorded the adhesion force of a single *Paracoccus seriniphilus* cell as a function of the contact time between cell and a glass surface (see Fig 8). Whereas an increase of the adhesion force with the contact time was already shown elsewhere when *Paracoccus seriniphilus* is immobilized by polydopamine [25], we used the FluidFM for immobilization. To counteract the effect of decreasing adhesion forces with an increasing number of force-distance curves, we measured with increasing and subsequently

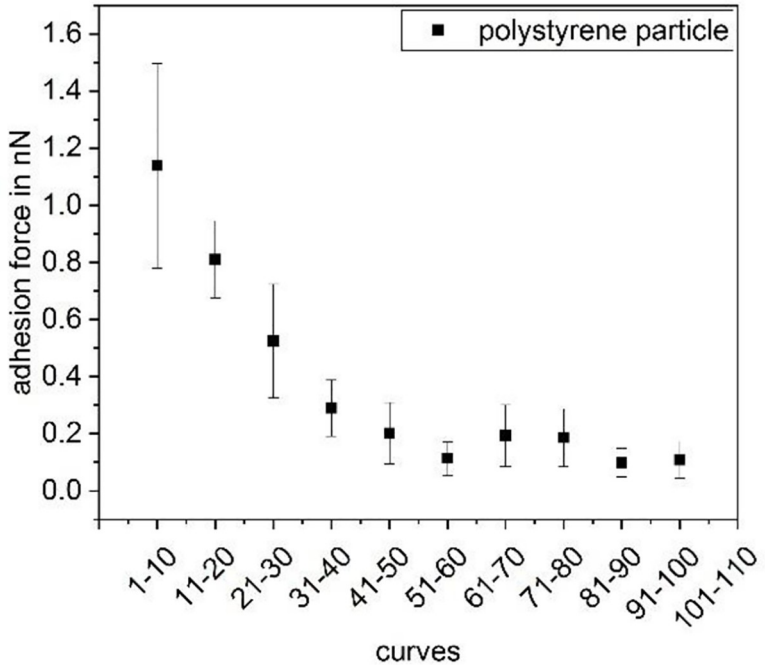

Fig 7. Adhesion force of a polystyrene particle as a function of the number of force-distance curves recorded previously.

https://doi.org/10.1371/journal.pone.0227395.g007

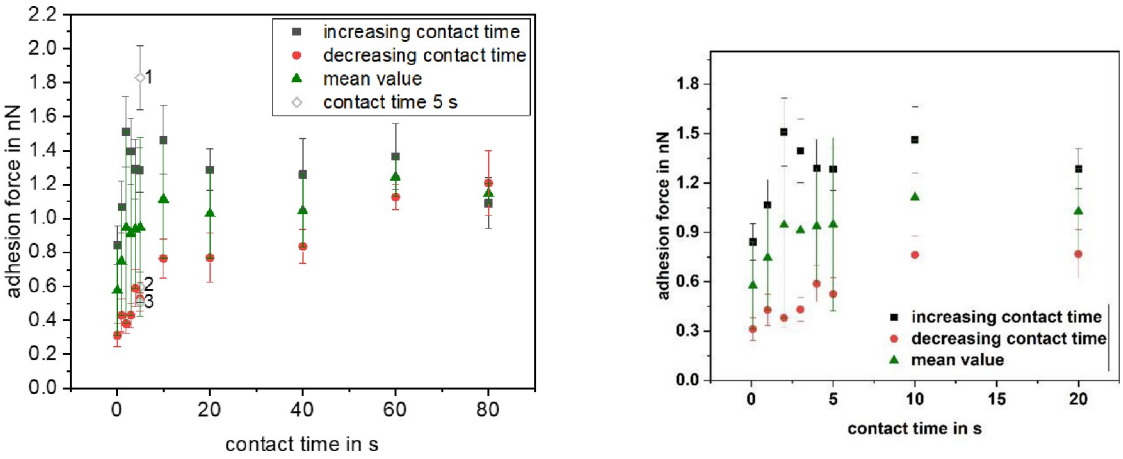

Fig 8. Influence of the contact time on the adhesion force of a single *Paracoccus seriniphilus* cell on glass. Each data point represents 15 force-distance curves. The data points depicted with void diamond at 5 s contact time were recorded at the beginning of the measurement (1), between the increasing and the decreasing contact times (2) and at the end of the measurement (3). On the right a zoom of the contact times up to 20 s is shown.

https://doi.org/10.1371/journal.pone.0227395.g008

decreasing contact times, thereby using the same cell. Especially in the beginning of the first measurement set, shown in black squares, the increase of the adhesion force due to an increasing contact time is strongly counteracted by the decrease due to the increasing number of recorded curves. This effect can be reduced by looking at the mean value of both measurement sets (triangles). However, the effect cannot be compensated completely.

Comparison between the immobilization of *Paracoccus seriniphilus* bacteria by polydopamine and FluidFM for SCFS

To assess if the immobilization with the FluidFM leads to different results compared to the conventional immobilization method using polydopamine, we investigated the adhesion force of *Paracoccus seriniphilus*, which is well-studied in terms of SCFS with polydopamine [25]. For this purpose, we compared the development of the adhesion forces of bacteria immobilized by the FluidFM with bacteria immobilized by means of the chemical functionalization of the cantilever with polydopamine.

Fig 9 shows the progression of the adhesion force of *Paracoccus seriniphilus* for multiple force-distance curves on glass, polished titanium and polished stainless steel, immobilized by polydopamine and FluidFM as well as a corresponding force-distance curve for both immobilization methods. 180 to 250 force-distance curves were recorded on one position on each surface, stainless steel being an exception in a way that the position was changed twice. For all cells and surfaces, the adhesion force of the bacterium decreases with a growing number of force-distance curves per position, regardless of the immobilization method. However, the extend of the decrease varies due to the individual cell that is used for the measurement. For example, the adhesion force decreases roughly linear on glass for both immobilization methods, as well as for one of the investigated cells on titanium if the cell is immobilized by FluidFM. On the other hand, the decrease on stainless steel is more pronounced within the first 100 force-distance curves. Further, since each data point is composed of ten force-distance curves, the adhesion force also decreases within the data points. The steeper decrease in the beginning of the measurement therefore causes higher error bars for the first data points compared to those of the data points recorded towards the end of the measurement. Fig 10 shows

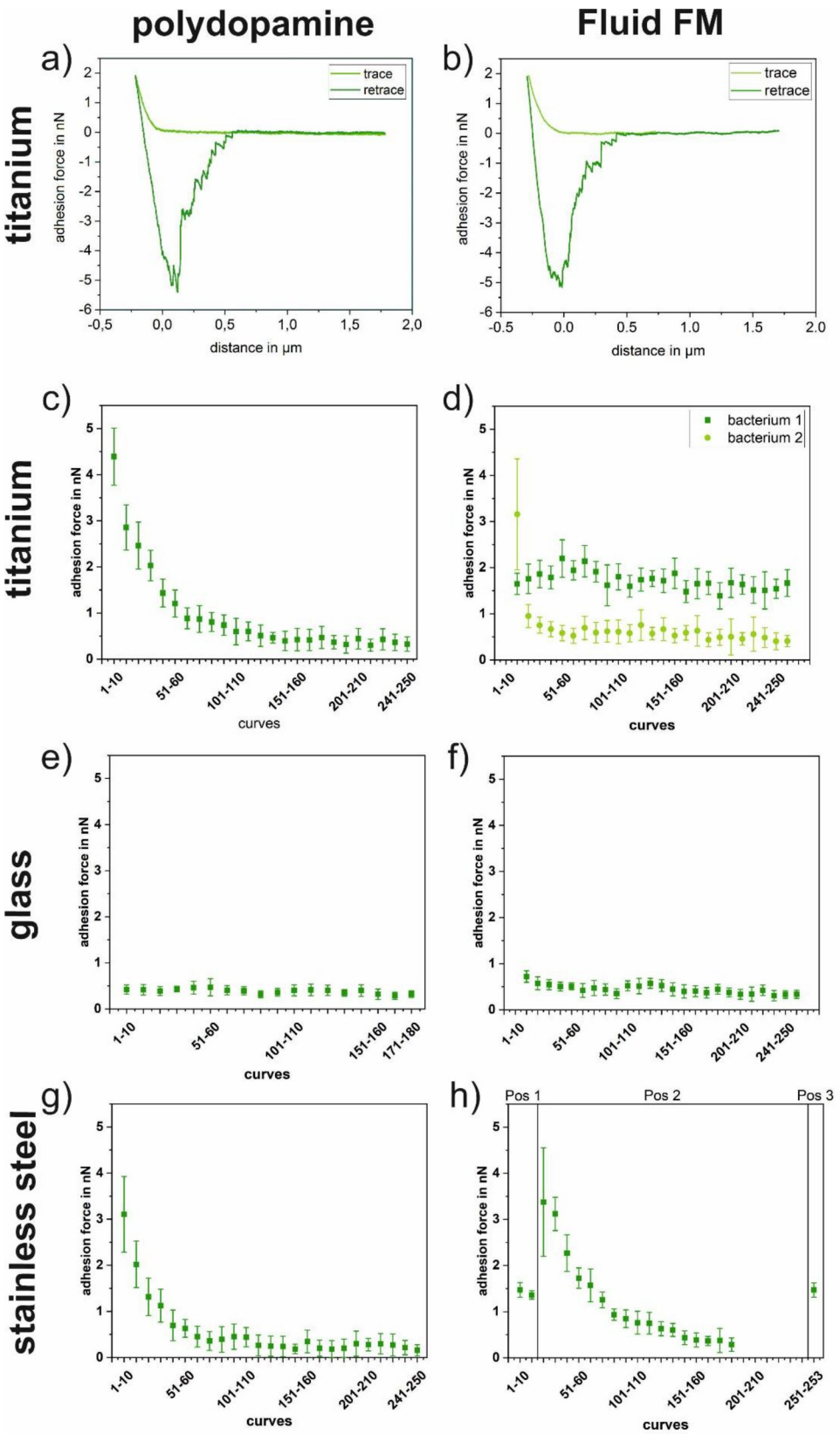
polydopamine
Fluid FM
a)
b)
c)
d)
e)
f)
g)
h)
titanium
titanium
glass
stainless steel
trace
retrace
adhesion force in nN
distance in µm
bacterium 1
bacterium 2
curves
Pos 1
Pos 2
Pos 3

Fig 9. Typical force distance curves of *Paracoccus seriniphilus* (a on titanium and b on glass). Adhesion forces (c-hof *Paracoccus seriniphilus* on glass, titanium and stainless steel. The cell is immobilized on the cantilever either by polydopamine (left) or using the FluidFM approach (right). If not marked otherwise, all underlying force-distance curves of each plot were recorded on the same position. Measurement parameters were: Setpoint 2 nN, z-length 2 μm, z-speed 2 μm/s, pause time 5s.

https://doi.org/10.1371/journal.pone.0227395.g009

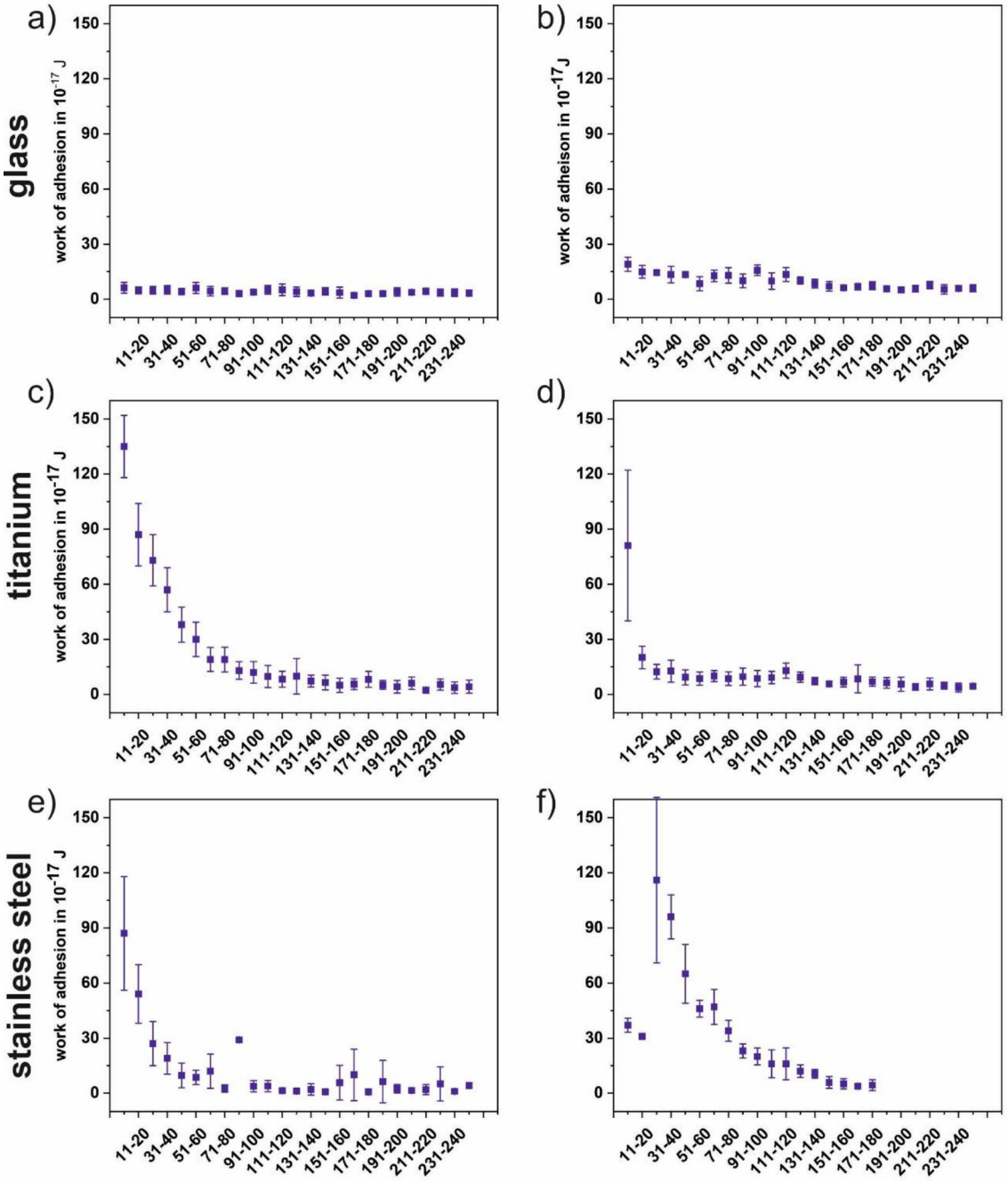

Fig 10. Work of adhesion of *Paracoccus seriniphilus* on glass. (a and b), titanium (c and d) and stainless steel (e and f) corresponding to the adhesion force measurements in Fig 9. The cell is immobilized on the cantilever either by polydopamine (left) or using the FluidFM approach (right). Measurement parameters were: Setpoint 2 nN, z-length 2 μm, z-speed 2 μm/s, pause time 5 s. For titanium only bacterium 2 from Fig 9 is shown here.

https://doi.org/10.1371/journal.pone.0227395.g010

the progression of the work of adhesion corresponding to the adhesion forces of Fig 9. For all surfaces the observations correspond to the trend described for the adhesion forces.

Further, taking into account the strong gradient between the data points in the beginning of the measurement set in Fig 7 and comparing them to the measurements on glass in Fig 9, these data supports the hypothesis that the different progression types observed in Fig 9 (linear and stronger in the beginning) are due to the use of different cells rather than to the immobilization method or the underlying substrate. Nevertheless, changes in the bacterial cells do not cause the changes solely. In Fig 9F, where the position was changed twice in the course of the measurement, a partial recovery of the original force value is observed, meaning that not only the bacterium but also the surface itself is lastingly influenced.

As for the comparison between the immobilization with polydopamine and FluidFM, the absolute force values and the work of adhesion values (see Fig 10) are in the same range and it cannot be distinguished between both immobilization methods in this setup. Further, the force-distance curves look similar for both methods.

Conclusions

We studied the influence of measurement parameters on FluidFM experiments and further showed that the results of a FluidFM experiment with a single bacterial cell lead to similar results compared to the conventional approach using polydopamine for immobilization. For a blank nanopipette, the adhesion force on a flat glass surface increases with the setpoint and when applying a suction force, whereas the z-speed shows no distinct influence.

We investigated the influence of the parameters setpoint, z-length, z-speed, pause time, and applied pressure on the shape and quality of force-distance curves of a single bacterial cell recorded by FluidFM. We found the adhesion force as well as the quality of the force-distance curves improve using higher setpoints in the range between 2 and 20 nN. Further, to obtain curves of good quality, a small z-length and a high z-speed should be applied. The applied underpressure had only a minor effect on the adhesion force of the cells. Even though the optimal parameters might differ using different bacterial strains, these general trends can help to find optimal parameters.

Further, we showed that the FluidFM is an appropriate and convenient method for the immobilization of *Lactococcus lactis*, a lactic acid bacterium that could not be immobilized reliably by conventional chemical functionalizations of the cantilever before. Further, by means of the well-studied *Paracoccus seriniphilus*, we showed that the physical immobilization using underpressure to hold the bacterium in place leads to the determination of adhesion forces similar to those obtained when applying polydopamine for immobilization. The reversible immobilization by the FluidFM allows for a quick change of cells and therefore enables to study a larger number of cells in less time compared to conventional chemical immobilization. Further, the FluidFM can be applied to immobilize various sorts of spherical bacteria, regardless of their outer membrane's composition.

For the FluidFM as well as for polydopamine, we observed a continuous decrease of the adhesion force of a single cell with a growing number of force-distance curves, complicating the comparison between different environmental parameters in terms of adhesion forces and resulting from changes both of the cell and the underlying surface.

Author Contributions

Conceptualization: Christiane Ziegler.

Funding acquisition: Christiane Ziegler.

Investigation: Linda Hofherr.

Resources: Christiane Ziegler.

Supervision: Christine Müller-Renno, Christiane Ziegler.

Writing – original draft: Linda Hofherr, Christiane Ziegler.

Writing – review & editing: Christine Müller-Renno, Christiane Ziegler.

References

1. Zhang L, Zhou S, Zhuang L, Li W, Zhang J, Lu N, et al. Microbial fuel cell based on Klebsiella pneumoniae biofilm. Electrochem commun. 2008; 10(10): 1641–1643.
2. Nicolella C, van Loosdrecht MC, Heijnen SJ. Particle-based biofilm reactor technology. Trends Biotechnol. 2000; 18(7): 312–320. https://doi.org/10.1016/s0167-7799(00)01461-x PMID: 10856927
3. Bühler K, Schmid A. Neue mikrobiologische Wege in der Chemie. BIOspektrum. 2011; 17(5): 528.
4. Kang S, Elimelech M. Bioinspired single bacterial cell force spectroscopy. Langmuir. 2009; 25(17): 9656–9659. https://doi.org/10.1021/la902247w PMID: 19634872
5. Beaussart A, El-Kirat-Chatel S, Sullan RMA, Alsteens D, Herman P, Derclaye S, et al. Quantifying the forces guiding microbial cell adhesion using single-cell force spectroscopy. Nat protoc. 2014; 9(5): 1049. https://doi.org/10.1038/nprot.2014.066 PMID: 24722404
6. Beaussart A, El-Kirat-Chatel S, Herman P, Alsteens D, Mahillon J, Hols P, et al. Single-cell force spectroscopy of probiotic bacteria. Biophys J. 2013; 104(9): 1886–1892. https://doi.org/10.1016/j.bpj.2013.03.046 PMID: 23663831
7. Bolshakova AV, Kiselyova OI, Filonov AS, Frolova OY, Lyubchenko YL, Yaminsky IV. Comparative studies of bacteria with an atomic force microscopy operating in different modes. Ultramicroscopy. 2001; 86(1–2): 121–128. https://doi.org/10.1016/s0304-3991(00)00075-9 PMID: 11215614
8. Schär-Zammaretti P, Ubbink J. The cell wall of lactic acid bacteria: surface constituents and macromolecular conformations. Biophys J. 2003; 85(6): 4076–4092. https://doi.org/10.1016/S0006-3495(03)74820-6 PMID: 14645095
9. Vadillo-Rodríguez V, Busscher HJ, Norde W, De Vries J, Dijkstra RJ, Stokroos I, et al. Comparison of atomic force microscopy interaction forces between bacteria and silicon nitride substrata for three commonly used immobilization methods. Appl Environ Microbiol. 2004; 70(9): 5441–5446. https://doi.org/10.1128/AEM.70.9.5441-5446.2004 PMID: 15345431
10. Meyer RL, Zhou X, Tang L, Arpanaei A, Kingshott P, Besenbacher F. Immobilisation of living bacteria for AFM imaging under physiological conditions. Ultramicroscopy. 2010; 110(11): 1349–1357. https://doi.org/10.1016/j.ultramic.2010.06.010 PMID: 20619542
11. Zeng G, Müller T, Meyer RL. Single-cell force spectroscopy of bacteria enabled by naturally derived proteins. Langmuir. 2014; 30(14): 4019–4025. https://doi.org/10.1021/la404673q PMID: 24654836
12. Razatos A, Ong YL, Sharma MM, Georgiou G. Molecular determinants of bacterial adhesion monitored by atomic force microscopy. PNAS. 1998; 95(19): 11059–11064. https://doi.org/10.1073/pnas.95.19.11059 PMID: 9736689
13. Sheng X, Ting YP, Pehkonen SO. Force measurements of bacterial adhesion on metals using a cell probe atomic force microscope. J colloid interface sci. 2007; 310(2): 661–669. https://doi.org/10.1016/j.jcis.2007.01.084 PMID: 17321534
14. Meister A, Gabi M, Behr P, Studer P, Vörös J, Niedermann P., et al. FluidFM: combining atomic force microscopy and nanofluidics in a universal liquid delivery system for single cell applications and beyond. Nano letters, 2009; 9(6): 2501–2507. https://doi.org/10.1021/nl901384x PMID: 19453133
15. Cohen N, Sarkar S, Hondroulis E, Sabhachandani P, Konry T. Quantification of intercellular adhesion forces measured by fluid force microscopy. Talanta. 2017; 174: 409–413. https://doi.org/10.1016/j.talanta.2017.06.038 PMID: 28738600
16. Sancho A, Vandersmissen I, Craps S, Luttun A, Groll J. A new strategy to measure intercellular adhesion forces in mature cell-cell contacts. Scientific reports. 2017; 7: 46152. https://doi.org/10.1038/srep46152 PMID: 28393890
17. McGrath J S, Quist J, Seddon J R, Lai S C, Lemay S G, Bridle H L. Deformability assessment of waterborne protozoa using a microfluidic-enabled force microscopy Probe. PloS one. 2016; 11(3).
18. Dörig P, Ossola D, Truong A M, Graf M, Stauffer F, Vörös J, et al. Exchangeable colloidal AFM probes for the quantification of irreversible and long-term interactions. Biophysical journal. 2013; 105(2): 463–472. https://doi.org/10.1016/j.bpj.2013.06.002 PMID: 23870267

19. Potthoff E, Ossola D, Zambelli T, Vorholt J A. Bacterial adhesion force quantification by fluidic force microscopy. Nanoscale. 2015; 7(9): 4070–4079. https://doi.org/10.1039/c4nr06495j PMID: 25660231

20. Sprecher K S, Hug I, Nesper J, Potthoff E, Mahi M A, Sangermani M., et al. Cohesive properties of the Caulobacter crescentus holdfast adhesin are regulated by a novel c-di-GMP effector protein. MBio. 2017; 8(2): e00294–17. https://doi.org/10.1128/mBio.00294-17 PMID: 28325767

21. Mittelviefhaus M, Müller D B, Zambelli T, Vorholt J A. A modular atomic force microscopy approach reveals a large range of hydrophobic adhesion forces among bacterial members of the leaf microbiota. The ISME journal. 2019; 13(7): 1878–1882. https://doi.org/10.1038/s41396-019-0404-1 PMID: 30894689

22. Kuipers OP, Beerthuyzen MM, de Ruyter PG, Luesink EJ, de Vos W. Autoregulation of nisin biosynthesis in Lactococcus lactis by signal transduction. J Biol Chem. 1995; 270(45): 27299–27304. https://doi.org/10.1074/jbc.270.45.27299 PMID: 7592991

23. Pukall R, Laroche M, Kroppenstedt RM, Schumann P, Stackebrandt E, Ulber R. Paracoccus seriniphilus sp. nov., an L-serine-dehydratase-producing coccus isolated from the marine bryozoan Bugula plumosa. Int J Syst Evol Micr. 2003; 53(2): 443–447.

24. Hofherr L, Chodorski J, Müller-Renno C, Ulber R, Ziegler C. Comparison of Versatile Immobilization Methods for Gram-Positive Bacteria on a Silicon Cantilever. phys status solidi (a). 2018; 215(15): 1700846.

25. Davoudi N, Huttenlochner K, Chodorski J, Schlegel C, Bohley M, Müller-Renno C, et al. Adhesion forces of the sea-water bacterium Paracoccus seriniphilus on titanium: Influence of microstructures and environmental conditions. Biointerphases, 2017; 12(5): 05G606. https://doi.org/10.1116/1.5002676 PMID: 29108418

26. Davoudi N, Müller-Renno C, Ziegler C, Raid I, Seewig J, Schlegel C, et al. Nanomechanical properties of the sea-water bacterium Paracoccus seriniphilus—A scanning force microscopy approach. Biointerphases. 2015; 10(1): 019004. https://doi.org/10.1116/1.4906862 PMID: 25708634

27. Fingerle M, Köhler O, Rösch C, Kratz F, Scheibe C, Davoudi N., et al. Cleaning of titanium substrates after application in a bioreactor. Biointerphases. 2015; 10(1): 019007. https://doi.org/10.1116/1.4907754 PMID: 25708637

28. Huttenlochner K, Müller-Renno C, Ziegler C, Merz R, Merz B, Kopnarski M., et al. Removing biofilms from stainless steel without changing surface properties relevant for bacterial attachment. Biointerphases, 2017; 12(2): 02C404. https://doi.org/10.1116/1.4982196 PMID: 28446023

29. Butt HJ, Jaschke M. Calculation of thermal noise in atomic force microscopy. Nanotechnology. 1995; 6 (1): 1.

30. Hutter JL, Bechhoefer J. Calibration of atomic-force microscope tips. Rev Sci Instrum. 1993; 64(7): 1868–1873.

31. Alfano JC, Carter PW, Dunham AJ, Nowak MJ, Tubergen KR. Polyelectrolyte-iduced aggregation of microcrystalline cellulose: reversibility and shear effects. J colloid interf sci 2000; 223(2): 244–254.